

MYELOID NEOPLASIA

EVI1 drives leukemogenesis through aberrant ERG activation

Johannes Schmoellerl,^{1,2,*} Inês A. M. Barbosa,^{1,3,*} Martina Minnich,¹ Florian Andersch,¹ Leonie Smeenk,^{4,5} Marije Havermans,^{4,5} Thomas Eder,² Tobias Neumann,¹ Julian Jude,¹ Michaela Fellner,¹ Anja Ebert,¹ Monika Steininger,^{1,3} Ruud Delwel,^{4,5} Florian Grebien,^{2,†} and Johannes Zuber^{1,6,†}

¹Research Institute of Molecular Pathology, Vienna BioCenter, Vienna, Austria; ²Institute for Medical Biochemistry, University of Veterinary Medicine Vienna, Vienna, Austria; ³Vienna BioCenter PhD Program, Doctoral School of the University of Vienna and Medical University of Vienna, Vienna, Austria; ⁴Department of Hematology, Erasmus Medical Center Cancer Institute, Rotterdam, The Netherlands; ⁵Oncode Institute, Utrecht, The Netherlands; and ⁶Medical University of Vienna, Vienna, Austria

KEY POINTS

- Comparative transcriptomics and genome-wide CRISPR screens identify conserved transcriptional programs and dependencies in EVI1-driven AML.
- ERG is the key transcriptional target of EVI1 that is required and sufficient for maintaining an immature differentiation state.

Chromosomal rearrangements involving the MDS1 and EVI1 complex locus (MECOM) on chromosome 3q26 define an aggressive subtype of acute myeloid leukemia (AML) that is associated with chemotherapy resistance and dismal prognosis. Established treatment regimens commonly fail in these patients, therefore, there is an urgent need for new therapeutic concepts that will require a better understanding of the molecular and cellular functions of the ecotropic viral integration site 1 (EVI1) oncogene. To characterize gene regulatory functions of EVI1 and associated dependencies in AML, we developed experimentally tractable human and murine disease models, investigated the transcriptional consequences of EVI1 withdrawal in vitro and in vivo, and performed the first genome-wide CRISPR screens in EVI1-dependent AML. By integrating conserved transcriptional targets with genetic dependency data, we identified and characterized the ETS transcription factor ERG as a direct transcriptional target of EVI1 that is aberrantly expressed and selectively required in both human and murine EVI1-driven AML. EVI1 controls the expression of ERG and occupies a conserved intragenic enhancer region in AML cell lines and samples from patients with primary AML. Suppression of ERG induces terminal differentiation of EVI1-driven AML cells, whereas ectopic expression of ERG abrogates their dependence on EVI1, indicating that the major oncogenic functions of EVI1 are mediated through aberrant transcriptional activation of ERG. Interfering with this regulatory axis may provide entry points for the development of rational targeted therapies.

Introduction

Chromosomal rearrangements leading to overexpression of EVI1 (MECOM) on chromosome 3q26 define a subtype of acute myeloid leukemia (AML) that is associated with chemoresistance and a 2-year survival of <10%.¹⁻³ Originally identified as common insertion site in retrovirally induced murine leukemias,⁴ the MECOM locus encodes multiple isoforms of the ecotropic viral integration site 1 (EVI1) transcription factor.⁵ In normal hematopoiesis, expression of EVI1 is restricted to hematopoietic stem cells (HSCs) and is critically required for maintaining a self-renewing, undifferentiated state.^{6,7} In AML, chromosomal rearrangements such as inv(3)(q21.3q26.2) or t(3;3)(q21.3;q26.2) juxtapose a distal GATA2 enhancer with the EVI1 promoter⁸⁻¹⁰ that drives aberrant expression of EVI1 through recruitment of hematopoietic transcription factors such as MYB, C/EBPα, and RUNX1.^{11,12} Other translocations such as t(3;21)(q26;q22) lead to the expression of RUNX1-EVI1 fusion proteins, whereas

t(3;8)(q26;q24) hijacks a MYC super-enhancer to drive aberrant EVI1 expression.¹³ Overexpression of EVI1 is also observed in the absence of structural rearrangements in certain AML subtypes, where it is similarly associated with poor prognosis.¹⁴⁻¹⁶

Although genetic events and gene regulatory mechanisms driving aberrant expression of EVI1 are increasingly well characterized, its molecular functions and downstream targets remain incompletely understood. The EVI1 protein contains 2 clusters of zinc finger domains that are separated by a repressive domain that harbors binding sites for corepressors, such as the C-terminal binding protein 1/2 (CTBP1/2).^{17,18} EVI1 is thought to control lineage-defining transcription factors in myelopoiesis such as PU.1 and C/EBPα.^{19,20} In addition, EVI1 has recently been shown to attenuate p53-mediated stress responses and thereby promote therapy resistance.²¹ However, owing to a lack of suitable experimental models, the precise makeup of EVI1-controlled transcriptional programs and their

functional contribution to leukemogenesis have remained largely elusive. Using a panel of tetracycline-mediated conditional disease models that recapitulate the phenotypic and transcriptional hallmarks of EVI1-driven AML, we have characterized EVI1-dependent transcriptional programs and performed a first panel of genome-wide CRISPR screens that uncover critical downstream targets and dependencies in EVI1-driven AML. We identify the ETS transcription factor, *ERG*, as a conserved transcriptional target of EVI1 that mediates stem cell-like transcriptional programs and is critically required for maintaining an immature cell state in EVI1-driven AML.

Methods

Statistics

For CRISPR screens, Gene Ontology (GO) term analyses, RNA sequencing (RNA-seq), assay for transposase-accessible chromatin using sequencing (ATAC-seq), chromatin immunoprecipitation DNA sequencing (ChIP-seq) and gene set enrichment analyses published statistical packages were used as referenced in the respective methods sections. For Pearson correlation of *ERG* vs *EVI1* expression values in patients with AML, the `cor.test()` function of the `stats` (version 4.2.0) R package was used. For Kaplan-Meier analyses, log-rank test was used. For single group comparisons of normalized gene expression values, mean fluorescence intensity and surface marker expression, 2-tailed Student *t* test was used for *P* value determination. **P* < .05, ***P* < .01, ****P* < .001, *****P* < .0001.

Patient material

Samples were collected from the Erasmus Medical Center Hematology Department biobank (Rotterdam, The Netherlands). Leukemic blasts were purified from bone marrow (BM) or blood by standard diagnostic procedures. Patient provided written informed consent in accordance with the Declaration of Helsinki. The medical ethical committee of the Erasmus Medical Center approved usage of the patient material for this study.

All other methods are described in detail in the supplemental Methods (available on the *Blood* website).

Results

Genome-wide CRISPR screen in human EVI1-dependent AML cells

To characterize disease-relevant targets of EVI1, we reasoned that a suitable cell line model should harbor a chromosome 3 rearrangement, aberrantly express and strictly depend on EVI1, parameters that can be assessed through genomic profiling and functional genetic screening data that are available for hundreds of human cell lines.²²⁻²⁹ Among 121 hematopoietic cell lines that have been interrogated using CRISPR/CRISPR-associated protein 9 (Cas9)- or RNA interference (RNAi)-based screens, we identified 20 EVI1-expressing cell lines (supplemental Figure 1A). To our surprise, *EVI1* was not identified as an essential gene in any CRISPR screen, whereas RNAi screens revealed HNT-34 as the only cell line that depends on *EVI1* (Figure 1A-B). To validate these findings, we transduced HNT-34 and 4 additional AML cell lines (KASUMI-3, MOLM-1, TF-1, HEL) that are commonly used as models for EVI1-driven AML^{10,30-32} with *EVI1*-targeting shRNAs (supplemental Figure 1B-H). Although knockdown of *MYC* was

detrimental in all tested AML cell lines, knockdown of *EVI1* strongly impaired proliferation only in HNT-34 cells (Figure 1C; supplemental Figure 1D-E), indicating that HNT-34 cells are uniquely suited for exploring transcriptional and genetic determinants in EVI1-dependent AML.

The HNT-34 cell line is composed of immature, CD34-expressing blasts that harbor 2 chromosomal translocations: t(3;3)(q21;q26) leading to a rearranged GATA2 enhancer driving aberrant *EVI1* expression and t(9;22)(q34;q11) that causes expression of the BCR/ABL1 fusion protein and was very likely acquired as a secondary event during disease progression.³³ We transduced HNT-34 cells with vectors enabling Dox-inducible expression of Cas9 (iCas9),³⁴ isolated single-cell-derived clones, validated tightly Dox-controllable and efficient genome editing, and confirmed the strong dependency of HNT-34 cells on *EVI1* (supplemental Figure 2A-F). To identify selective dependencies in EVI1-driven AML, we performed parallel genome-wide CRISPR/Cas9 screens in HNT-34 and 2 MLL/AF9-driven AML cell lines (MOLM-13, THP-1) that are not addicted to *EVI1* (supplemental Table 1). iCas9-expressing HNT-34, MOLM-13, and THP-1 cells were transduced with the Vienna single guide RNA (sgRNA) library,³⁵ and changes in sgRNA representation were measured after 14 population doublings. To benchmark the performance of our screening system, we compared dropout effects of core essential genes in iCas9 MOLM-13 cells to 3 published screens in the same cell line (supplemental Figure 2G)^{23,25,26} and found that the median effect size was between 15- and 49-fold higher in our analysis (Figure 1D; supplemental Figure 2H). To leverage this high dynamic range for the identification of context-specific dependencies, we compared screening results in HNT-34 and MOLM-13 cells. Among 578 genes that were strongly depleted in MOLM-13 but not in HNT-34 cells, we identified several known cofactors and mediators of MLL fusion-driven leukemogenesis, such as *MEN1*, *ZFP64*, *SIK3*, and *CEBPA*,³⁶⁻³⁹ as well as *FLT3*, a known driver in MOLM-13 cells.⁴⁰ Conversely, 124 genes were selectively required in HNT-34 but not in MOLM-13 cells, including *EVI1*, both components of BCR/ABL1, and *GATA2* (Figure 1E). In GO analysis, HNT-34-specific dependencies were enriched for genes involved in stem cell differentiation, hematopoiesis, and cell cycle regulation, whereas MOLM-13 cells displayed unique vulnerabilities in genes involved in translational elongation, histone acetylation, and nucleosome organization (Figure 1E-F).

Because HNT-34 cells represent the only EVI1-dependent AML cell line that has been interrogated in genome-wide CRISPR screens, we reasoned that comparing our results to available genome-wide screens in other AML cell lines could help to further delineate EVI1-specific dependencies. Indeed, many genes that were selectively required in HNT-34 cells in comparison to MOLM-13 cells also showed no depletion in THP-1 and a broader panel of AML cell lines (supplemental Figure 2I-J). These putative EVI1-specific dependencies included several factors involved in stem cell biology, such as *ERG*, *ETV6*, and the *EVI1* interactor *CTBP2*.^{17,18,41-43} Together, these functional analyses show that HNT-34 cells recapitulate principal EVI1-associated dependencies and thus can be used to investigate its regulatory functions and associated vulnerabilities.

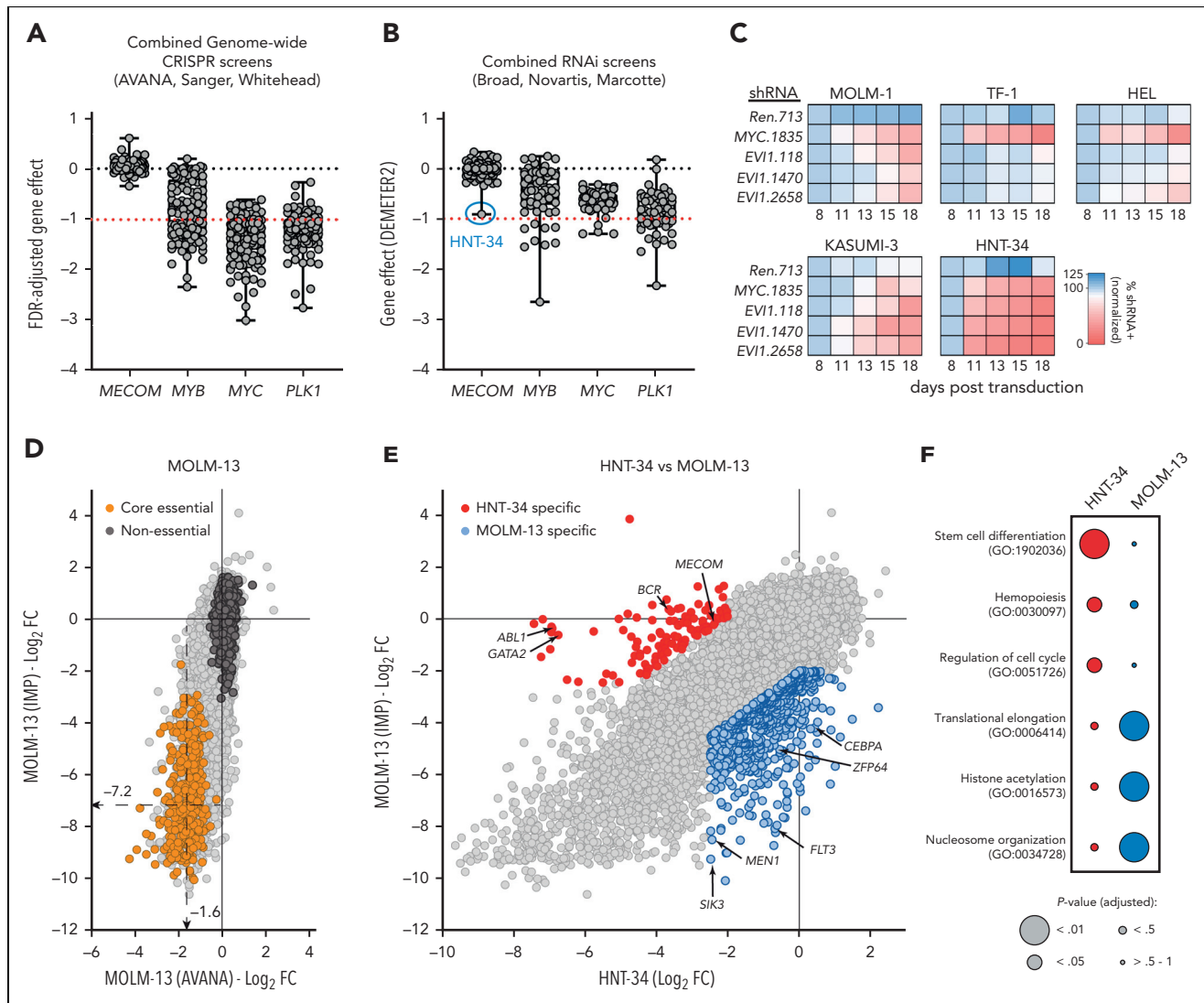


Figure 1. Identification of human EVI1-dependent AML cell lines. (A) Reanalysis of CRISPR-based loss-of-function screens of 102 hematopoietic cell lines. Each dot represents a distinct screen. Gene effects were normalized to false discovery rate (FDR)-adjusted median effects size of defined core essential and nonessential genes. (B) Reanalysis of RNAi-based loss-of-function screens of 61 hematopoietic cell lines retrieved from the Cancer Dependency Map (depmap.org). Each dot represents a distinct screen. Gene effects are normalized using DEMETER2.²⁹ (C) Competitive proliferation assay in human AML cell lines. Illustrated as color-coded percentage of dsRed-positive cells expressing indicated short hairpin RNAs (shRNAs) over 18 days. The nontargeting shRNA Ren.713 is used as negative control and the MYC-targeting shRNA as positive control. Results are normalized to day 8 after transduction and are shown as the mean of 3 biological replicates. (D) Comparative analysis of 2 CRISPR-based loss-of-function screens in MOLM-13 cells using the data set of this study (Institute of Molecular Pathology [IMP]) and the publicly available Avana data set.²⁶ Gray dots represent all genes. Axis shows enrichment/depletion as log₂ fold change (FC). Orange dots represent genes defined as core essential, whereas dark gray dots represent nonessential genes. Dashed lines indicate median log₂-fold depletion of core essential genes. (E) Comparative analysis of CRISPR-based loss-of-function screens of HNT-34 vs MOLM-13 cells. Red dots represent genes that selectively impair HNT-34 cells upon knockout (log₂ FC in HNT-34 < -2, at least 2 log₂ difference compared with MOLM-13 and log₂ FC in MOLM-13 > -2.5). Blue dots represent genes that selectively impair MOLM-13 cells upon knockout (log₂ FC < -2 in MOLM-13, at least 2 log₂ difference compared with HNT-34, and log₂ FC in HNT-34 > -2.5). (F) GO term analysis of genes with selective effects within HNT-34 compared with MOLM-13.

Mouse models recapitulate human EVI1-driven AML

Because human cell lines are prone to artifacts and unsuitable for studying gene functions *in vivo*, we sought to complement our analyses in HNT-34 cells with studies in a genetically engineered mouse model of EVI1-driven AML. Overexpression of EVI1 or RUNX1/EVI1 in murine hematopoietic stem and progenitor cells (mHSPCs) induces myelodysplasia in syngeneic recipient mice that can progress to bona fide AML with long latencies,⁴⁴⁻⁴⁶ suggesting that additional driver events are required. Because

human EVI1-rearranged AML most commonly harbor mutations in RAS signaling components, we sought to combine a RUNX1/EVI1 fusion gene⁴⁶ with oncogenic *Nras*^{G12D}, which is known to cooperate with *Evi1* and other oncogenic fusion proteins in murine leukemogenesis.⁴⁷⁻⁴⁹ To be able to suppress RUNX1/EVI1 in established AML *in vivo*, we adapted a Dox-repressible (Tet-OFF) expression system⁴⁸ that is based on 2 retroviral constructs, one encoding RUNX1/EVI1 and GFP under the control of a tetracycline-responsive promoter (TRE3G) and the other delivering constitutively expressed *Nras*^{G12D}, luciferase, and the tetracycline transactivator (tTA) (Figure 2A). Syngeneic recipient

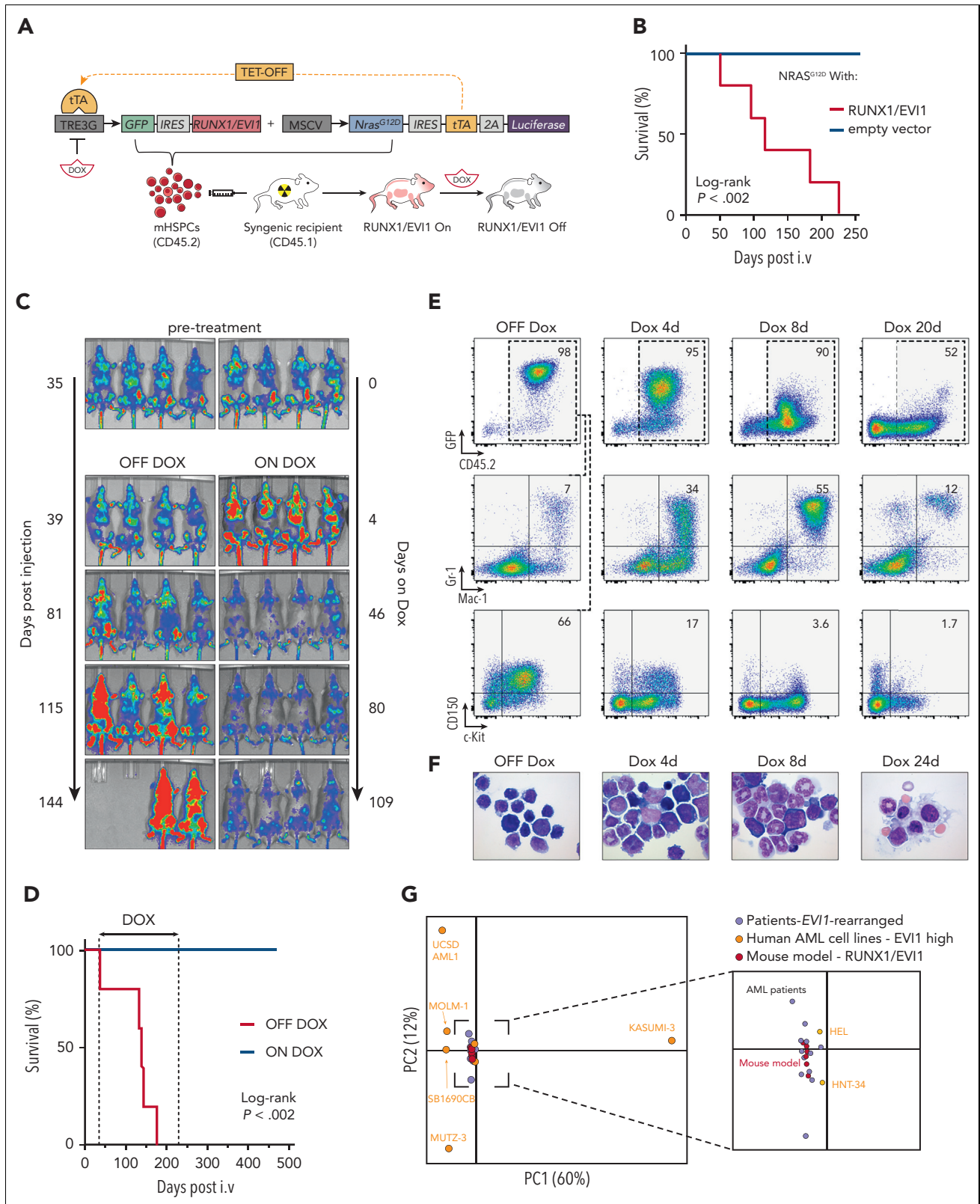


Figure 2. Development of preclinical models of EVI1-rearranged AML. (A) Schematic outline of the generation of a transplantation-based RUNX1/EVI1-driven mouse model allowing controllable oncogene expression. (B) Kaplan-Meier survival analysis of mice transplanted with mHSPCs expressing Nras^{G12D} combined with either vector control or RUNX1/EVI1 ($n \geq 5$). (C) Bioluminescence imaging of mice transplanted with RUNX1/EVI1-expressing leukemia cells that received either Dox treatment (4 mg/mL) or regular drinking water. (D) Kaplan-Meier survival analysis of mice transplanted with RUNX1/EVI1-expressing leukemia cells that received Dox treatment (4 mg/mL) compared with untreated controls ($n = 5$). (E) Flow cytometric analyses of BM-derived leukemia cells of mice transplanted with RUNX1/EVI1-expressing leukemia cells that received Dox treatment (4 mg/mL) compared with untreated controls. Relative amounts of GFP⁺CD45.2⁺ donor cells were quantified and further characterized toward their immunophenotype. (F) BM cytopsin of mice transplanted with RUNX1/EVI1-expressing leukemia cells at indicated time points upon Dox treatment (4 mg/mL) compared with untreated controls. (G) Principal component analysis of the gene expression of human EVI1-expressing AML cell lines ($n = 7$), human patients with AML harboring EVI1 rearrangements ($n = 12$) and murine leukemia models expressing RUNX1/EVI1 ($n = 6$).

mice of mHSPC cotransduced with both vectors developed an AML-like disease with a mean survival of 116 days (Figure 2B). The BM of diseased animals was dominated by immature GFP⁺ blasts expressing high levels of the HSC markers CD150 and c-Kit, but it also contained more differentiated GFP⁺ cells coexpressing myeloid markers (supplemental Figure 3A).

The RUNX1/EV11;Nras^{G12D}-induced leukemias were transplantable into secondary recipients and remained highly dependent on RUNX1/EV11 expression. Withdrawal of the fusion protein led to disease regression that was stable even after discontinuing Dox, and none of the Dox-treated animals succumbed to leukemia over an observation period of 468 days (Figure 2C-D). Upon Dox treatment, GFP⁺ RUNX1/EV11 leukemia cells gradually lost surface expression of CD150 and c-Kit and differentiated into Mac-1/Gr-1-expressing myeloid cells (Figure 2E-F). These effects were not observed when RUNX1/EV11 was expressed from a constitutive promoter in an otherwise identical model (supplemental Figure 3B), demonstrating that leukemia regression was caused by loss of RUNX1/EV11 and not by unrelated Dox effects.⁵⁰ Interestingly, at an early time point (4 days of Dox treatment), we observed a transient increase in leukemia burden (Figure 2C), suggesting that withdrawal of RUNX1/EV11 initially enhances cell proliferation. To investigate this further, we determined the cell cycle state of leukemia cells after 3 and 5 days of Dox treatment using 5-bromo-2'-deoxyuridine (BrdU)/7AAD labeling in vivo (supplemental Figure 4A). Indeed, Dox-treated leukemia cells showed an increase in BrdU incorporation and a higher fraction of cells in S-phase (supplemental Figure 4B-E), suggesting that RUNX1/EV11 withdrawal releases slowly cycling blasts into a differentiation program that initially involves a transient amplification of myeloid progenitors, reminiscent of early steps during myeloid differentiation.^{51,52}

To investigate whether typical transcriptional states of human EV11-driven AML are recapitulated in our RUNX1/EV11;Nras^{G12D}-driven mouse model, we analyzed the transcriptomes of ex vivo-isolated leukemia cells by messenger RNA (mRNA) sequencing and compared them to RNA-seq profiles of EV11-rearranged human AML cell lines and primary patient samples.^{10,53-57} Among AML cell lines, only HNT-34 and HEL cells clustered closely together with RNA-seq profiles from samples from patient with primary EV11-rearranged AML in principal component analyses, whereas other EV11-expressing AML cell lines had substantially deviated in their transcriptional state (Figure 2G). By contrast, RUNX1/EV11;Nras^{G12D}-driven AML mouse models closely resembled transcriptional states of EV11-rearranged AML in patients and thus provide suitable models for studying this disease.

To enable functional genetic studies using Dox-inducible RNAi or CRISPR/Cas9, we generated a version of our mouse model that coexpresses a reverse tTA 3 (rtTA3) (supplemental Figure 3C). Disease phenotypes precisely mirrored other RUNX1/EV11;Nras^{G12D}-AML models (supplemental Figure 3D-E), and we were able to expand leukemia cells in culture, where they retained their immature phenotype and dependence on RUNX1/EV11 (supplemental Figure 3F-G).

EV11 regulates a conserved set of transcriptional targets in human and murine AML

To characterize gene regulatory functions of EV11 in vivo, we transplanted leukemia cells driven by Dox-repressible

RUNX1/EV11 and Nras^{G12D} into secondary recipients and profiled the transcriptome in steady state and upon Dox-mediated repression of RUNX1/EV11 (Figure 3A). Dox treatment strongly suppressed the expression of RUNX1/EV11 and GFP, whereas Nras^{G12D} was unaffected (supplemental Figure 5A). Overall, suppression of RUNX1/EV11 in vivo resulted in 942 downregulated and 915 upregulated genes (supplemental Figure 5B), whereas Dox treatment of the constitutive RUNX1/EV11;Nras^{G12D}-driven model caused deregulation of only 21 genes (supplemental Figure 5A-B). As an orthogonal approach, we performed RNA-seq upon RNAi-mediated suppression of RUNX1/EV11 in cultured rtTA3-expressing leukemia cells, which altered the expression of 1341 genes, 514 of which overlapped with changes observed after RUNX1/EV11 suppression in our Dox-repressible model in vivo (Figure 3A-C). To further delineate critical EV11 targets that are conserved between species, we compared the response to EV11 suppression in our mouse model to transcriptional effects observed upon shRNA-mediated knockdown of EV11 in HNT-34 cells (supplemental Figure 5C-F; supplemental Table 2). In GO term analyses, genes involved in cytokine response and hematopoiesis were upregulated and downregulated, respectively, to similar degrees in culture and in vivo (Figure 3D). Regulators of intracellular signaling were distinct between cultured cells and in vivo, whereas regulators of cell migration and adhesion were in vivo specific, indicating that EV11 fulfills important functions in microenvironmental interactions that are not captured in culture.

To identify critical EV11 targets that are conserved between species and in vivo and in vitro culture, we compared the response to EV11 suppression in our mouse models to transcriptional effects observed upon shRNA-mediated knockdown of EV11 in HNT-34 cells. This intersection revealed a core set of 35 upregulated and 33 downregulated context- and species-independent EV11 target genes (Figure 3E), in line with its proposed dual function as a transcriptional activator and a repressor. Genes commonly upregulated upon EV11 suppression included the cell cycle regulators CDK6 and CCND3, which may promote the transient amplification of myeloid progenitors observed upon EV11 withdrawal in our mouse model (supplemental Figure 4). Genes that were commonly downregulated upon EV11 suppression included several transcription factors and transcriptional coregulators (ie, *BCL11A*, *CBX6*, *ERG*, *HHEX*, and *LYL1*), and this core set of EV11-dependent transcripts was significantly enriched in patients with EV11-rearranged AML as compared with other AML subtypes (Figure 3F; supplemental Figure 5G-H). This suggests that EV11 controls a limited set of conserved transcriptional target genes that are prime candidates for mediating its oncogenic functions.

ERG is a transcriptional target of EV11 that is selectively required in EV11-driven AML

To systematically explore the functional relevance of conserved transcriptional targets and other EV11-associated dependencies, we complemented our genome-wide CRISPR screen in HNT-34 cells with a similar screen in our RUNX1/EV11;Nras^{G12D}-driven mouse model (Figure 2G). We introduced the mouse version of the Vienna sgRNA library³⁵ into Cas9-expressing RUNX1/EV11;Nras^{G12D} AML cells and determined the representation of sgRNAs after 14 population doublings (supplemental Figure 6A). To distinguish EV11-associated from more broadly relevant AML

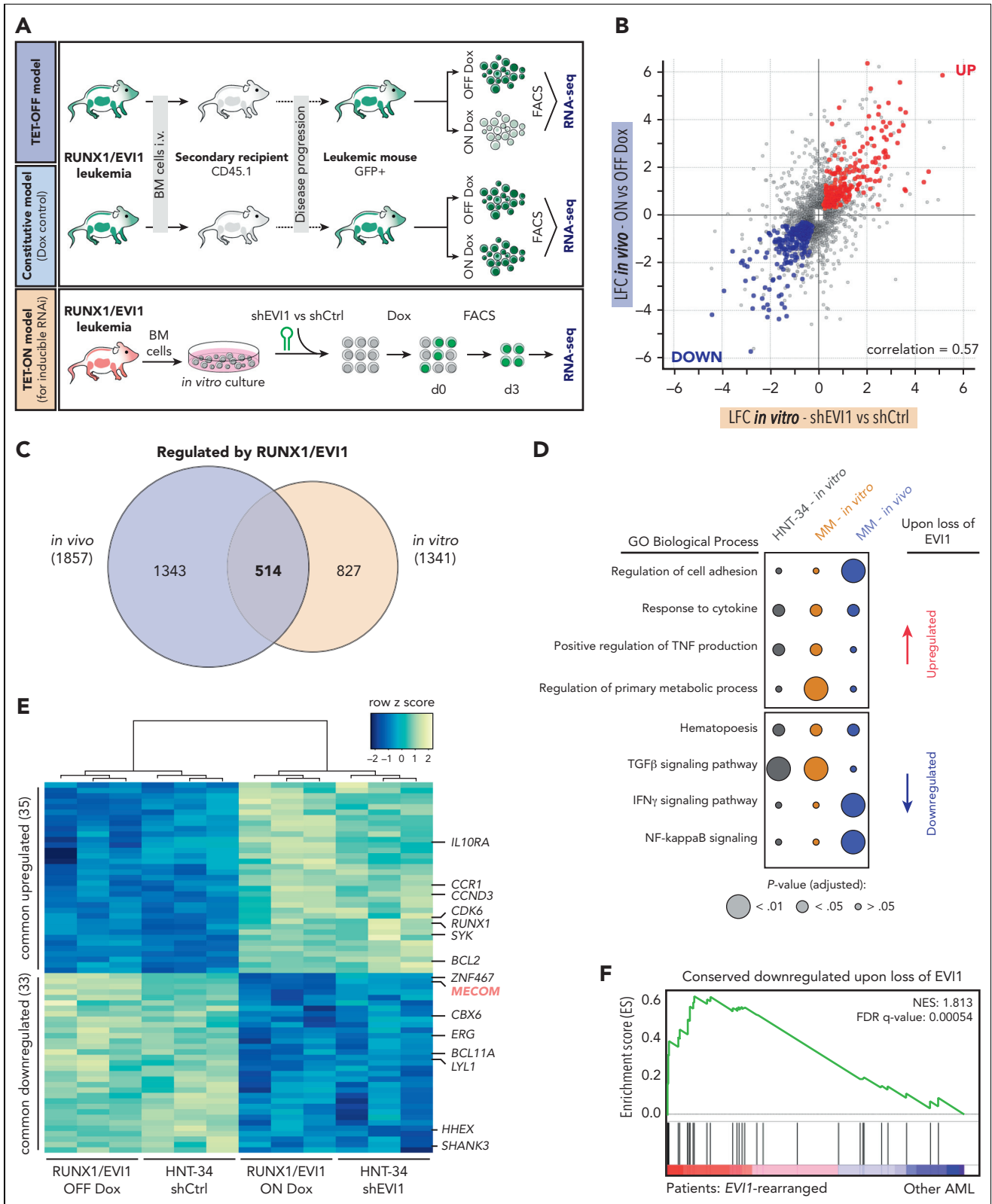


Figure 3. EVI1 regulates a common core of transcriptional targets in human and murine AML. (A) Schematic outline of the workflow to investigate RUNX1/EVI1-dependent transcriptional programs. For in vivo studies, GFP-positive leukemia cells from primary recipient animals driven by *Nras*^{G12D} and regulatable (TET-OFF model) or constitutive RUNX1/EVI1 (Dox control model) were transplanted into secondary recipients. After initial engraftment, mice were treated with Dox (4 mg/mL) for 3 days or kept untreated. GFP⁺CD45.2⁺cKit⁺Mac1⁻ cells were sorted, and gene expression was analyzed by RNA-seq ($n \geq 3$). For in vitro studies, BM-derived leukemia cells driven by constitutive RUNX1/EVI1, *Nras*^{G12D} and expressing rTA3 (TET-ON model) were cultivated and biological triplicates of cells were transduced with inducible shRNA vectors targeting RUNX1/EVI1 (shEVI1.2658) or nontargeting (shRen.713) control. Gene expression was analyzed upon purifying cells by fluorescence-activated cell sorter 3 days post Dox-mediated (0.5 µg/mL) GFP/shRNA induction. (B) Scatter plot showing log₂-FCs (LFCs) of significantly deregulated (adjusted $P < .05$) genes (gray dots) in leukemia cells 3

dependencies, we performed a parallel screen in an established MLL/AF9;Nras^{G12D}-driven AML mouse model.⁵⁸ Both screens clearly separated core essential and nonessential genes (supplemental Figure 6B; supplemental Table 3), and their comparison revealed numerous selective dependencies in RUNX1/EVI1;Nras^{G12D}-driven AML, several of which were also detected in HNT-34 cells, such as the transcriptional regulators *Gata2*, *Erg*, *Etv6*, and *Runx3* (supplemental Figure 6C).

From the core set of 33 conserved transcriptionally activated targets of EVI1, only 3 transcription factors, *Bcl11a*, *Erg*, and *Hhex*, were required in murine RUNX1/EVI1;Nras^{G12D}-driven AML cells (Figure 4A). Further integration of genome-wide CRISPR screening data revealed the ETS-related transcription factor ERG as the only gene that represents both a conserved transcriptional target and a context-specific dependency in human and murine EVI1-dependent AML (Figure 4A-B).

To probe the relevance of ERG and other EVI1-associated dependencies beyond our models, we integrated our and other data sets from high-quality CRISPR screens in human and murine AML cell lines^{23,25-27} and determined selective dependencies associated with specific driver mutations. To benchmark this approach, we first extracted selective dependencies in a group of 8 MLL-rearranged AML cell lines. Among top-scoring MLL-associated dependencies, we identified several factors that are known to be required for MLL fusion protein-driven leukemogenesis, such as *MEN1*, *SRPK1*, *ZFP64*, and *SIK3*^{36,37,59,60} (supplemental Figure 6D). Applying this systematic approach to EVI1-dependent AML cell lines identified ERG as the most prominent selective dependency (Figure 4C).

These findings prompted us to further investigate the role of ERG as a critical downstream target of EVI1. Suppression of EVI1 in human HNT-34 and murine RUNX1/EVI1;Nras^{G12D}-driven AML cells led to a strong reduction of ERG mRNA and protein levels (Figure 4D-F). To investigate whether these effects are based on a direct role of EVI1 in ERG transcription, we determined genomic EVI1-binding sites using ChIP-seq in 2 EVI1-rearranged AML cell lines and a primary patient sample. The ERG locus harbored prominent EVI1 binding sites in 2 intragenic regions that were consistently detected in all 3 samples and overlapped with enhancer-associated H3K27 acetylation marks and regions of accessible chromatin determined by ATAC-seq (Figure 4G). Further analyses revealed that this conserved EVI1-bound enhancer region represents the well-described ERG +85 enhancer that contributes to ERG regulation in healthy and leukemic cells.⁴³ Together with our expression data, this suggests that EVI1 directly drives ERG expression via interactions with 2 conserved enhancer elements.

To functionally validate the selective dependency of EVI1-driven AML cell lines on ERG, we suppressed ERG expression in HNT-34 and several EVI1-independent human AML cell lines

using Dox-inducible RNAi. In accordance with results from CRISPR screens, shRNA-mediated knockdown of ERG strongly impaired the proliferation of EVI1-driven HNT-34 cells, whereas EVI1-independent AML cell lines were unaffected (Figure 5A; supplemental Figures 6E-F and 7A-C). Similarly, CRISPR/Cas9-mediated knockout and shRNA-mediated knockdown of ERG had no effects on MLL/AF9;Nras^{G12D}-driven murine AML cells, whereas the proliferation of RUNX1/EVI1;Nras^{G12D}-driven AML cells was strongly impaired (Figure 5B; supplemental Figures 6G and 7D-F). These effects were accompanied by a reduction in c-Kit and an increase in Mac-1 surface expression levels (Figure 5C), morphological signs of myeloid differentiation (Figure 5D), and the induction of apoptosis (Figure 5E). Taken together, these results establish ERG as an important EVI1 target that is required for maintaining the immature state of EVI1-driven AML cells.

Major oncogenic effects of EVI1 are mediated through aberrant activation of ERG

To delineate the relationship and regulatory roles of EVI1 and ERG, we investigated dynamic changes in accessible chromatin upon EVI1 suppression in RUNX1/EVI1;Nras^{G12D}-driven AML cells using ATAC-seq. Genes that were downregulated upon knockdown of EVI1 showed a marked reduction in chromatin accessibility (Figure 6A). Regions with reduced accessibility upon EVI knockdown included several regions in the *Erg* locus (supplemental Figure 8A), further suggesting that EVI1 directly activates ERG transcription. To systematically explore transcription factors that might contribute to aberrant gene activation in EVI1-driven AML, we quantified transcription factor-binding motifs in differentially accessible regions of EVI1-dependent genes (Figure 6C). As expected, the consensus motif of EVI1 itself showed a strong enrichment (Figure 6D). The ERG motif was almost as strongly enriched as EVI1 in open chromatin sites around EVI1-dependent genes. Moreover, reanalysis of publicly available ERG ChIP-seq data^{61,62} revealed ERG-binding sites in many genomic regions within EVI1-regulated genes (Figure 6B), suggesting that a large fraction of EVI1-induced transcriptional effects is mediated via aberrant activation of ERG. Alternatively, ERG could represent an essential cofactor of EVI1-dependent transcriptional regulation.

To distinguish between these 2 scenarios, we asked whether ectopic ERG expression could restore the proliferation of AML cells in the absence of EVI1 (supplemental Figure 8B). In competitive proliferation assays, knockdown of either RUNX1/EVI1 or *Myc* strongly impaired the proliferation of AML cells. Strikingly, ectopic expression of ERG fully rescued the detrimental effects of EVI1 suppression, whereas sensitivity to *Myc* suppression was retained (Figure 6E). Moreover, restoration of ERG expression fully prevented the induction of myeloid differentiation upon EVI1 knockdown (Figure 6F-G), thus rescuing the prevalent phenotype of oncogene withdrawal in EVI1-driven AML.

Figure 3 (continued) days upon Dox-mediated RUNX1/EVI1 knockdown in vitro compared with nontargeting control (x-axis) vs Dox-mediated RUNX1/EVI1 repression in vivo (y-axis). Red dots represent commonly upregulated genes. Blue dots represent commonly downregulated genes. (C) Venn diagram illustrating significant (adjusted $P < .05$) transcriptional changes 3 days upon shRNA-mediated RUNX1/EVI1 knockdown in vitro and Dox-mediated RUNX1/EVI1 repression in vivo in murine leukemia cells. (D) GO term enrichment analyses of gene sets deregulated upon EVI1 or RUNX1/EVI1 shutdown in human and murine leukemia in vitro or in vivo. (E) Heatmap of the 68 commonly upregulated and downregulated genes of human HNT-34 cells upon EVI1 knockdown and BM-derived murine RUNX1/EVI1-driven leukemia cells upon Dox-mediated fusion protein repression (adjusted $P < .05$). (F) Gene set enrichment analysis illustrating the enrichment of the genes that are downregulated upon loss of EVI1 in human patients with AML with EVI1 rearrangements. IFN- γ , interferon gamma; NES, normal enrichment score; NF, nuclear factor; TGF β , transforming growth factor β ; TNF, tumor necrosis factor.

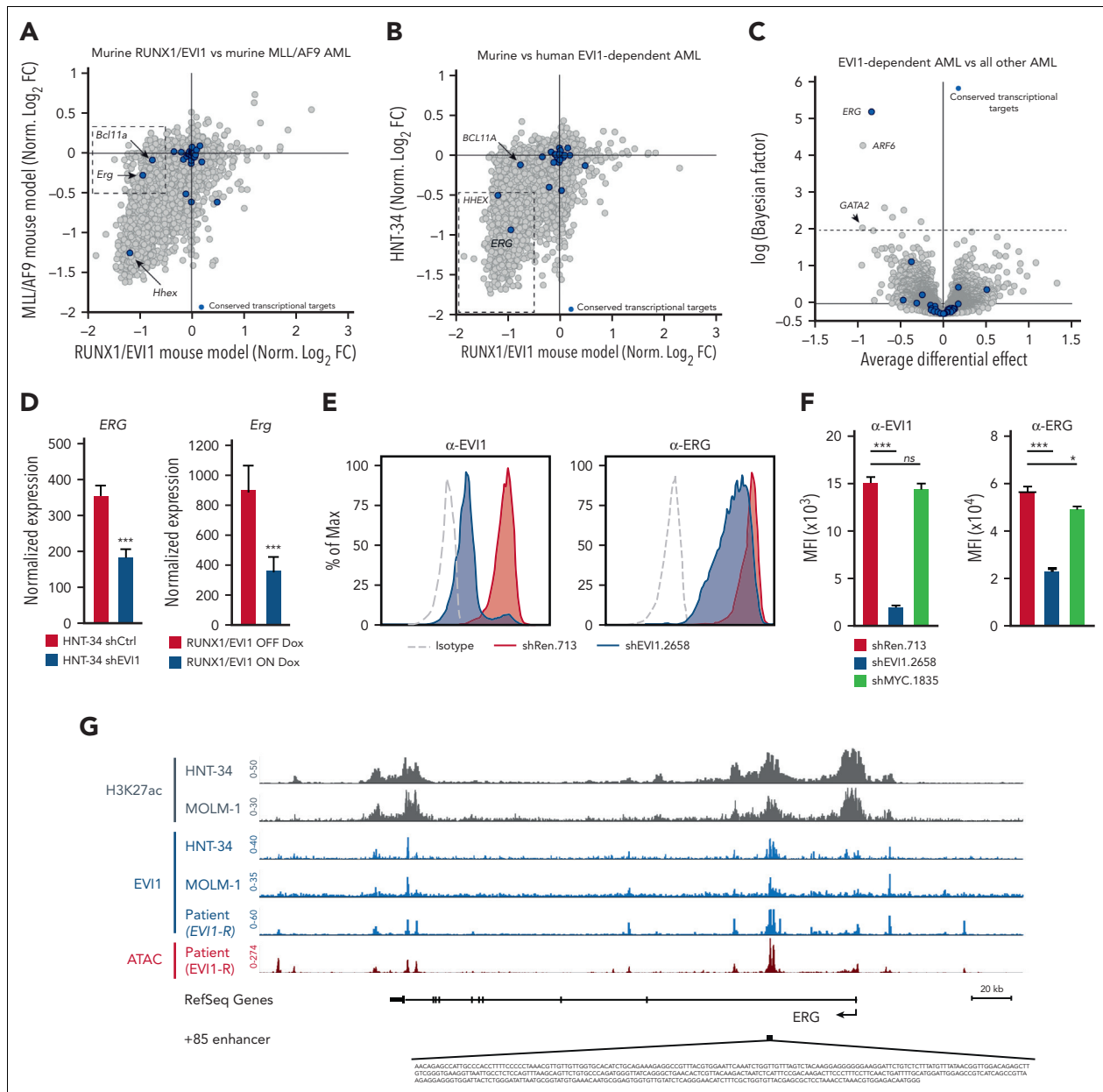
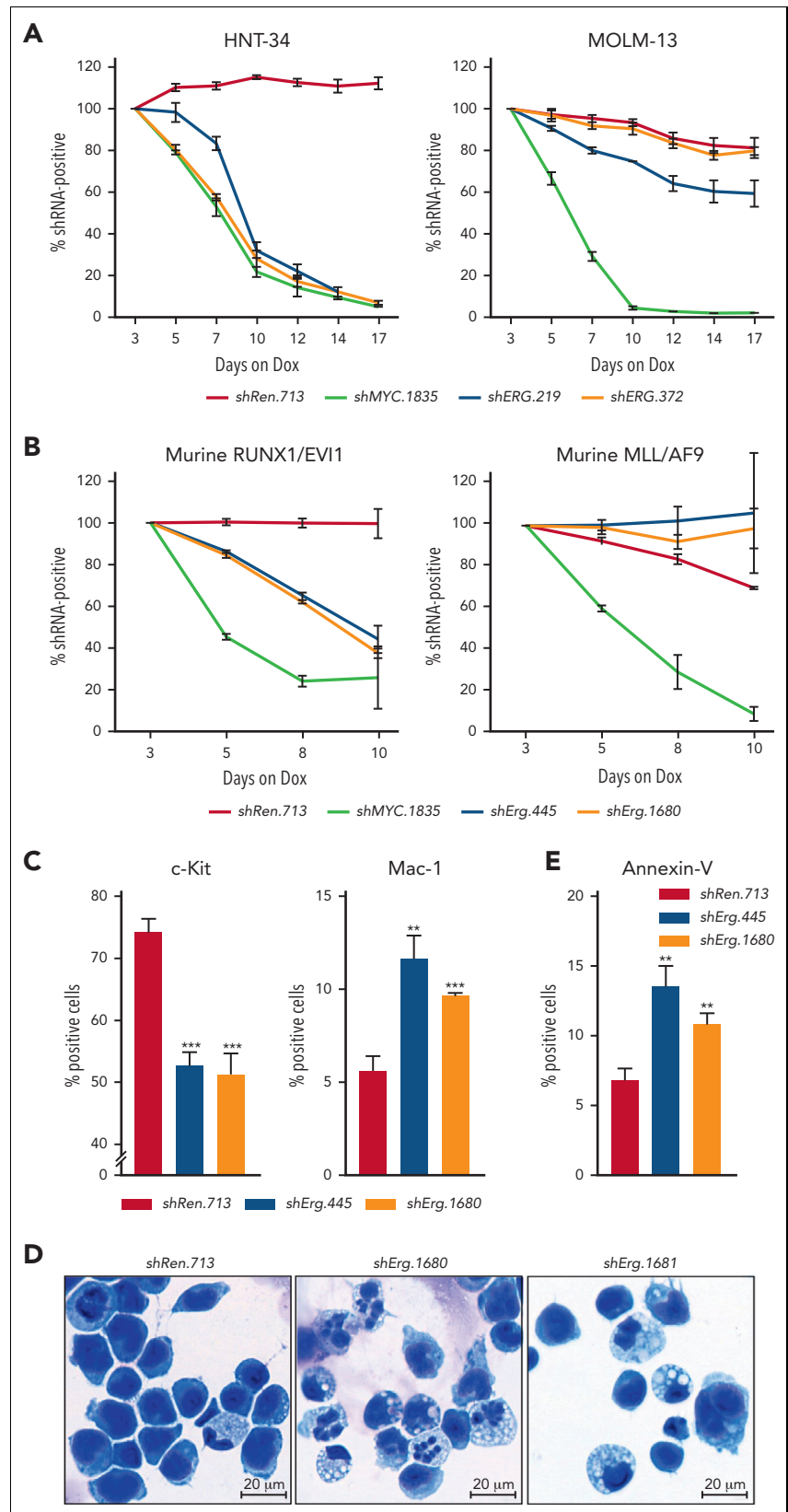


Figure 4. ERG is a direct transcriptional target of EVI1 in murine and human AML. (A) Genome-wide CRISPR/Cas9-based loss-of-function screens in murine RUNX1/EVI1 vs MLL/AF9-driven leukemia cells. Gray dots illustrate all genes. Dark blue dots represent conserved transcriptional targets of EVI1. Axis shows FDR-adjusted normalized log₂ FC. Dashed box represents genes with an FDR-adjusted normalized log₂ FC < -0.5 in murine RUNX1/EVI1-driven and > -0.5 in murine MLL/AF9-driven AML. (B) Genome-wide CRISPR/Cas9-based loss-of-function screens in murine RUNX1/EVI1-driven vs human HNT-34 AML cells. Gray dots illustrate all genes. Dark blue dots represent conserved transcriptional targets of EVI1. Axis shows FDR-adjusted normalized log₂ FC. Dashed box represents genes with an FDR-adjusted normalized log₂ FC < -0.5 in murine RUNX1/EVI1-driven AML and < -0.5 in human HNT-34 cells. (C) Comparative analysis of loss-of-function-mediated gene effects in human and murine EVI1-dependent AML compared with all other AML cell lines. Gray dots represent all genes. Dark blue dots represent conserved transcriptional targets of EVI1. X-axis depicts the average differential gene effect between the 2 groups. Y-axis depicts the log-transformed Bayesian factor. (D) Expression of ERG in human HNT-34 cells 5 days upon shRNA-mediated EVI1 knockdown in vitro and in murine ex vivo-derived RUNX1/EVI1-driven leukemia cells extracted from the BM of mice upon 3 days of Dox treatment (mean ± standard deviation [SD]; n = 3). (E) Flow cytometric analysis of intracellular RUNX1/EVI1 and ERG levels in murine leukemia cells 5 days upon RUNX1/EVI1 knockdown compared with nontargeting and isotype control. (F) Quantification of the mean fluorescence intensity of RUNX1/EVI1 and ERG levels as determined by flow cytometry in murine leukemia cells 5 days upon RUNX1/EVI1 knockdown, compared with knockdown of Myc and nontargeting shRen.713 (mean ± SD; n = 3). (G) EVI1 occupancy at the ERG locus. H3K27ac ChIP-seq in HNT-34 and MOLM-1 (gray). EVI1 ChIP-seq in HNT-34, MOLM-1 and primary patient-derived AML cells (EVI1-R, blue). ATAC-seq in patient-derived AML cells (red). The +85 stem cell enhancer region⁴³ is indicated. ns, not significant.

To characterize the ERG-dependent transcriptional program underlying these effects, we determined transcriptional changes following EVI1 withdrawal in the presence or absence of ectopically expressed ERG. Remarkably, ectopic expression of ERG rescued the expression of 34% of all genes that were

downregulated upon EVI1 withdrawal (supplemental Figure 8C; supplemental Table 4). ERG-dependent target genes included surface markers of hematopoietic stem and progenitor cells (*Slamf1*, *Kit*) and critical regulators of cancer cell proliferation and survival such as *Myc* and the MDM2-binding protein *Mtbp*

Figure 5. ERG is a selective dependency in EVI1-driven AML. Competitive proliferation assays, showing as the percentage of IRFP670-positive cells expressing indicated shRNAs over time. Nontargeting shRen.713 and essential shMYC.1835 were used as negative and positive controls, respectively (mean \pm SD; n = 3). (A) Competitive proliferation assay using human AML cell lines. (B) Competitive proliferation assay using RUNX1/EVI1-driven vs MLL/AF9-driven murine leukemia cells. (C) Flow cytometric analyses of murine RUNX1/EVI1-driven leukemia cells 7 days post Dox-mediated shRNA induction (mean \pm SD; n = 3). Quantification of c-Kit and Mac-1 surface marker expression. (D) Representative cytopsin images of purified murine RUNX1/EVI1-driven leukemia cells expressing indicated shRNAs 10 days post Dox-mediated shRNA induction. (E) Flow cytometric analyses of murine RUNX1/EVI1-driven leukemia cells 7 days post Dox-mediated shRNA induction (mean \pm SD; n = 3). Quantification of annexin V-positive cells.



(Figure 6H). In addition, several genes associated with hematopoietic differentiation that were induced upon EVI1 withdrawal (eg, *Pf4*, *Hemgn*, and *Cpox*) remained silent in the

presence of ectopically expressed ERG. A significant fraction of these rescued genes was also bound by ERG^{G1,62} (supplemental Figure 8D). Together, these data suggest that ERG controls an

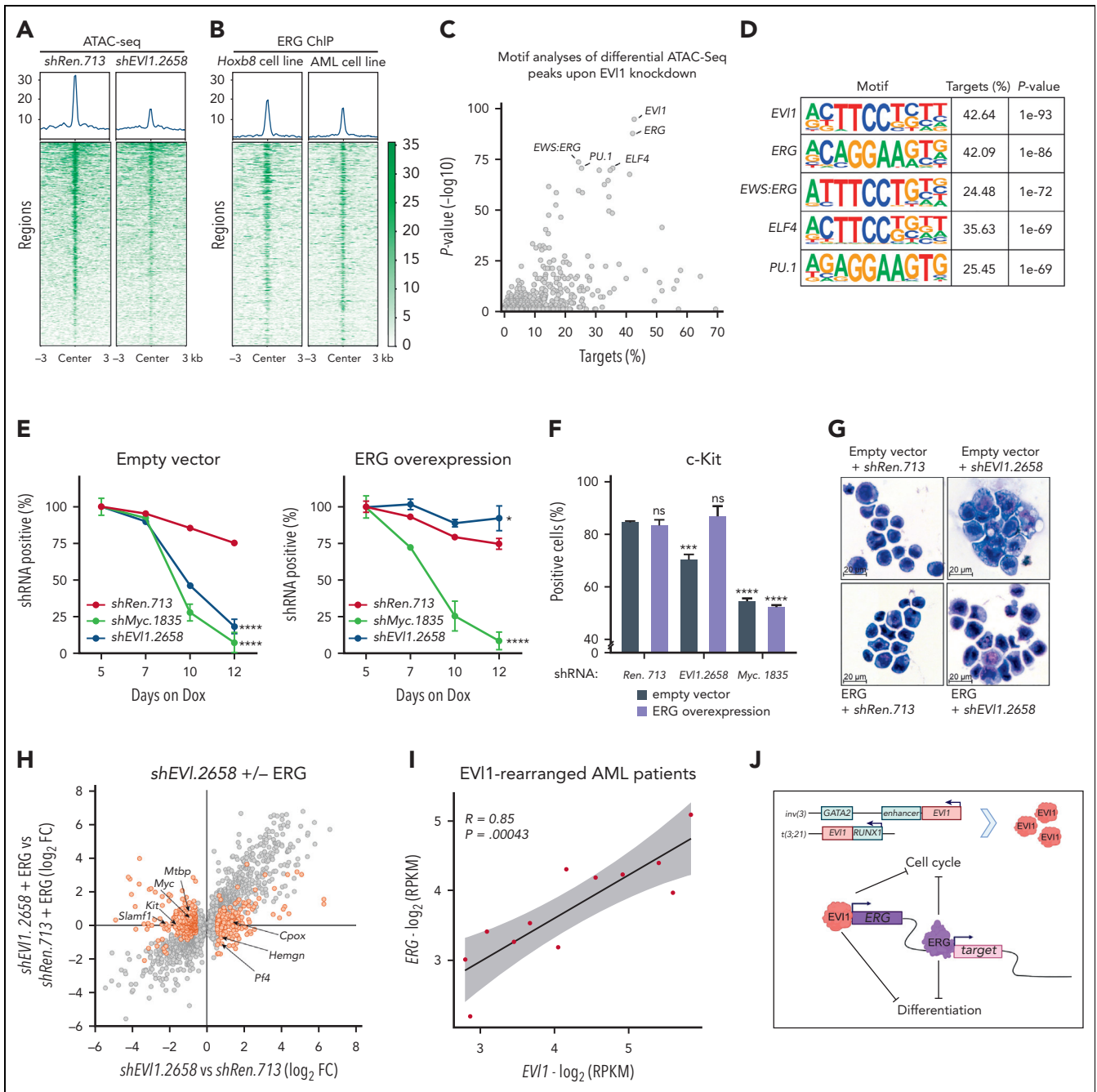


Figure 6. ERG is a critical mediator of EVI1-driven leukemogenesis. (A) Density maps of ATAC-seq peaks in murine RUNX1/EVI1 leukemia cells without (shRen.713) or with shRNA-mediated knockdown of EVI1 (shEVI1.2658); shown are RUNX1/EVI1 target genes that were found downregulated both upon shRNA-mediated RUNX1/EVI1 knockdown in vitro and upon Dox-mediated RUNX1/EVI1 withdrawal in vivo. (B) Density maps of ERG binding in reanalyzed ChIP-seq data from Hoxb8-expressing hematopoietic progenitor cells⁶¹ and murine MLL/AF9-driven leukemia cells⁶²; shown are the same genes as in panel A. (C) Transcription factor motif enrichment analysis within sequences of ATAC-seq peaks identified in panel A. Gray dots depict transcription factor motifs. The x-axis depicts the percentage of sequences with transcription factor motif. The y-axis depicts the (-log₁₀)-transformed P value significance compared with random background sequences. (D) Illustration of the top 5 enriched transcription factor motifs. (E) Knockdown-rescue studies of EVI1. Competitive proliferation assay of murine RUNX1/EVI1-driven leukemia cells expressing indicated shRNAs in the presence of Dox (0.5 μg/mL) that were cotransduced with either empty vector control (left) or ERG complementary DNA (right) (mean ± SD; n = 3). (F) Quantification of the progenitor marker c-Kit using flow cytometry in murine RUNX1/EVI1-driven leukemia cells 5 days post Dox-mediated shRNA induction (mean ± SD; n = 3). (G) Representative cytopsin images of murine RUNX1/EVI1-driven leukemia cells expressing indicated shRNAs and expression constructs. (H) Gene expression analysis 5 days upon RUNX1/EVI1 knockdown vs nontargeting control in the presence or absence of ectopic ERG expression. Gray dots illustrate genes with significantly changed expression (adjusted P < .1) upon RUNX1/EVI1 knockdown. Orange dots highlight rescued genes (opposing log₂ FC or adjusted P > .1) (n = 3). (I) Pearson correlation of EVI1 and ERG normalized expression values in human patients with AML with EVI1 rearrangements. (J) Proposed model of EVI1-driven leukemogenesis. Aberrant EVI1 expression, due to chromosomal rearrangements, drives aberrant ERG overexpression that blocks cellular differentiation and affects cell cycle regulation. RPKM, reads per kilobase million.

oncogenic transcriptional program downstream of EVI1 that is essential for the survival of EVI1-driven AML cells.

Given the regulatory relationship between EVI1 and ERG in our human and murine model systems, we analyzed a possible association of these genes in RNA-seq data from samples from patients with AML harboring *EVI1* rearrangements. Indeed, expression levels of EVI1 and ERG were highly correlated ($R = 0.85$, $P < .001$), indicating that EVI1 drives aberrant ERG expression also in primary human AML (Figure 6I). Collectively, our findings establish ERG as a key transcriptional target of EVI1 that mediates aberrant self-renewal and impaired cell differentiation in EVI1-driven leukemogenesis (Figure 6J).

Discussion

Genome-wide CRISPR screens have emerged as a powerful tool to systematically define essential genes in cancer cell lines and thereby uncover vulnerabilities that might be exploitable for therapy. Although this approach has been widely used to map context-specific dependencies in >100 leukemia cell lines,²²⁻²⁸ these so far excluded EVI1-dependent AML because of a lack of suitable cell culture models. Although our findings suggest that several commonly used cell line models of EVI1-driven AML have lost their dependency on EVI1, it remains to be determined whether such phenomena are cell culture artifacts or can occur in patients. Our study identifies and characterizes the AML cell line HNT-34, which harbors a t(3;3)(q21;q26) rearrangement³³ and has uniquely retained a strong dependency on EVI1, as a relevant and experimentally tractable human cell culture model.

As a complementary experimental system, we established a panel of RUNX1/EVI1;Nras^{G12D}-driven AML mouse models that recapitulate phenotypic and transcriptional states of human EVI1-rearranged AML and enable Tet-conditional functional genetic studies. In various configurations, RUNX1/EVI1 and Nras^{G12D} consistently induced an AML-like disease that was dominated by very immature blasts that retained stem cell-like properties, which may underly chemotherapy resistance and other characteristics of EVI1-rearranged AML.^{7,21,63} Withdrawal of RUNX1/EVI1 in vivo released immature blasts into a terminal differentiation program that involved an early phase of enhanced proliferation, which resembles the transition from quiescent HSCs to amplifying progenitor cells during normal hematopoiesis. This transition was accompanied by transcriptional activation of cell cycle regulators such as *CDK6* and *CCND3*, which was also observed following EVI1 suppression in human HNT-34 cells. It is tempting to speculate that leukemia cells entering this transient proliferative phase following EVI1 suppression are particularly vulnerable to cytostatic agents, suggesting that targeted therapies interfering with EVI1 could be rationally combined with conventional chemotherapy in a sequential manner. Cell cycle and microenvironmental effects of EVI1 might be further modulated by Ras pathway mutations or monosomy 7 with associated SAMD9/SAMD9L mutations,^{64,65} which both recently co-occur with EVI1-rearrangements in patients with AML.⁵⁴

Parallel genome-wide CRISPR screens in HNT-34 cells and an AML cell line derived from our RUNX1/EVI1; Nras^{G12D}-driven AML mouse model revealed several EVI1-associated dependencies that were not identified in our own and other published CRISPR-based dropout screens in EVI1-negative AML cell lines. Prominent EVI1-specific dependencies include

members of the CTBP transcriptional corepressor family, which are known interaction partners of EVI1,^{17,18} and the transcription factor GATA2, a master regulator in normal hematopoiesis. Interestingly, although haploinsufficiency of GATA2 is known to cooperate with aberrant EVI1 expression during leukemogenesis,^{9,10,66} its function is selectively required in human and murine EVI1-driven AML. Notably, our CRISPR screens in RUNX1/EVI1; Nras^{G12D}-driven AML did not detect a dependency on *Ckmt1*, which has been proposed as a candidate target in EVI1-driven AML.³² Our human CRISPR library, owing to a lack of gene-specific sgRNA predictions, only contained sgRNAs targeting one of the human paralogs, *CKMT1B*, which did not score in HNT-34 cells. We also could not detect expression of *CKMT1* genes in HNT-34 cells, our mouse models, or samples from patients with EVI1-rearranged AML used in our study, indicating that a dependency on *CKMT1* is not a generalizable feature of EVI1-driven AML.

Genes that were both commonly downregulated following EVI1 suppression and essential in human and murine EVI1-driven AML models included 3 transcription factors. BCL11A plays an important role in the regulation of globin gene expression⁶⁷ and has recently been shown to promote leukemogenesis by repressing PU.1 target genes.⁶⁸ The homeobox protein HHEX1 has been shown to repress the *Cdkn2a*-encoded tumor suppressors p16INK4a and p19ARF through recruitment of the polycomb repressive complex 2 and thereby promote MLL/ENL-driven leukemogenesis.⁶⁹ Although both BCL11A and HHEX1 appear to be more broadly implicated in leukemogenesis, the most prominent and selective EVI1-specific dependency turned out to be the ETS transcription factor ERG, which we characterized as a conserved transcriptional target of EVI1 in human and murine EVI1-driven AML.

In normal hematopoiesis, ERG is predominantly expressed in HSCs and, similar to EVI1, is known to be required for their maintenance by restricting differentiation.^{6,42,70} In AML, high expression of both EVI1 and ERG has been proposed as a molecular marker to stratify AML cases that derive from transformed HSCs as cell of origin and are associated with poor prognosis.^{16,71} Expression of FUS-ERG fusion proteins resulting from rare t(16;21) rearrangements is thought to promote AML through repression of retinoic acid signaling,^{72,73} whereas focal or large amplifications of chromosome 21 can lead to overexpression of ERG in diverse AML subtypes.^{74,75} Our data suggest that EVI1 commonly drives aberrant ERG expression in AML via its intragenic +85 enhancer, similar to what has been described for various oncogenes in T-cell acute lymphoblastic leukemia.⁷⁶ Supporting such a role, a complementary study by Masamoto et al. has identified ERG as an important transcriptional target of EVI1 through characterizing chromatin binding of Evi1 and transcriptional profiling in a newly generated mouse model.⁷⁷ Although several mechanisms can lead to aberrant ERG activation, a dependency on ERG is only observed in a few leukemia cell lines.^{26,78} Beyond leukemia, chromosomal rearrangements leading to aberrant expression of TMPRSS2/ERG fusion proteins are the most frequent driver events in human prostate cancer,⁷⁹ whereas EWS/ERG fusion proteins are major drivers of Ewing sarcoma.⁸⁰ Although the molecular functions of ERG fusion proteins and differentiation hierarchies remain incompletely understood in these tissues, it is tempting to speculate that aberrant ERG expression also arrests immature progenitor cells in these tumor types.

In EVI1-driven AML, our study uncovers ERG as a conserved and critical transcriptional target of EVI1 that is required and sufficient to arrest leukemia cells in a stem cell–like state. New classes of targeted therapeutics such as molecular glue degraders and protein interaction inhibitors provide a promising avenue for interfering with this unique regulatory relationship between EVI1 and ERG and thereby developing rational therapeutics that are urgently needed in EVI1-driven AML.

Acknowledgments

The authors thank all colleagues from the Zuber and Grebien groups for scientific discussions, Gerald Schmauss, Marietta Weninger, and Mario Nezhyba for expert fluorescence-activated cell sorting, and Pawel Pasierbek for imaging advice. The authors are grateful to the Molecular Biology Services as well as to the animal care takers at Institute of Molecular Pathology (IMP)/Institute of Molecular Biotechnology of the Austrian Academy of Sciences, and to Andreas Sommer and his team at the Vienna BioCenter Core Facilities (<https://www.vbcf.ac.at>) for deep sequencing services. The authors also thank Yosuke Masamoto and Mineo Kurokawa for scientific discussions and for sharing unpublished data and manuscript drafts.

This work was supported by starting grants from the European Research Council to (336860) (J.Z.) and to (636855) (F.G.), the Austrian Science Fund (SFB grant F4710) (J.Z.), a fellowship from the Daniel den Hoed, Erasmus Medical Center Foundation (L.S.), and the Koningin Wilhelmina Fonds grant from the Dutch Cancer Society (R.D.). J.S. is a recipient of a Doctoral Fellowship Programme of the Austrian Academy of Sciences. Research at the IMP is generously supported by Boehringer Ingelheim and the Austrian Research Promotion Agency (headquarter grant FFG-852936).

Authorship

Contribution: J.S., I.A.M.B., F.G., and J.Z. conceptualized the study; J.S., I.A.M.B., F.A., J.J., and J.Z. provided the methodology; J.S., I.A.M.B., M.M., F.A., L.S., M.H., T.E., T.N., J.J., M.F., A.E., M.S., R.D., F.G., and J.Z. performed the investigations; and J.S. and J.Z. wrote the manuscript with input from all coauthors.

Conflict-of-interest disclosure: J.Z. is a founder, shareholder, and scientific advisor of Quantro Therapeutics GmbH. J.Z. and the Zuber

laboratory receive research support and funding from Boehringer Ingelheim. The remaining authors declare no competing financial interests.

ORCID profiles: J.S., 0000-0002-8461-8881; I.A.M.B., 0000-0001-8977-0930; M.M., 0000-0003-4677-3300; L.S., 0000-0001-7025-8515; T.N., 0000-0003-3908-4224; J.J., 0000-0002-9091-9867; A.E., 0000-0002-2425-473X; F.G., 0000-0003-4289-2281; J.Z., 0000-0001-8810-6835.

Correspondence: Johannes Zuber, Research Institute of Molecular Pathology, Campus Vienna BioCenter 1, 1030 Vienna, Austria; email: johannes.zuber@imp.ac.at; and Florian Grebien, Institute for Medical Biochemistry, University of Veterinary Medicine Vienna, 1210 Vienna, Austria; email: florian.grebien@vetmeduni.ac.at.

Footnotes

Submitted 6 April 2022; accepted 28 August 2022; republished online on *Blood* First Edition 12 September 2022. <https://doi.org/10.1182/blood.2022016592>.

*J.S. and I.A.M.B. contributed equally to this study.

†J.Z. and F.G. contributed equally to this study.

The data reported in this article have been deposited in the Gene Expression Omnibus database (accession number GSE195497) and to the European Genome-Phenome Archive (accession number EGAS00001005959).

Data are available on request from the corresponding authors, Johannes Zuber (johannes.zuber@imp.ac.at) and Florian Grebien (florian.grebien@vetmeduni.ac.at).

The online version of this article contains a data supplement.

There is a [Blood Commentary](#) on this article in this issue.

The publication costs of this article were defrayed in part by page charge payment. Therefore, and solely to indicate this fact, this article is hereby marked “advertisement” in accordance with 18 USC section 1734.

REFERENCES

- Lugthart S, Gröschel S, Beverloo HB, et al. Clinical, molecular, and prognostic significance of WHO type inv(3)(q21q26.2)/t(3;3)(q21;q26.2) and various other 3q abnormalities in acute myeloid leukemia. *J Clin Oncol*. 2010;28(24):3890-3898.
- Papaemmanuil E, Gerstung M, Bullinger L, et al. Genomic classification and prognosis in acute myeloid leukemia. *N Engl J Med*. 2016;374(23):2209-2221.
- Wu X, Wang H, Deng J, et al. Prognostic significance of the EVI1 gene expression in patients with acute myeloid leukemia: a meta-analysis. *Ann Hematol*. 2019;98(11):2485-2496.
- Mucenski ML, Taylor BA, Ihle JN, et al. Identification of a common ecotropic viral integration site, Evi-1, in the DNA of AKXD murine myeloid tumors. *Mol Cell Biol*. 1988;8(1):301-308.
- Fears S, Mathieu C, Zeleznik-Le N, et al. Intergenic splicing of MDS1 and EVI1 occurs in normal tissues as well as in myeloid leukemia and produces a new member of the PR domain family. *Proc Natl Acad Sci U S A*. 1996;93(4):1642-1647.
- Kataoka K, Sato T, Yoshimi A, et al. Evi1 is essential for hematopoietic stem cell self-renewal, and its expression marks hematopoietic cells with long-term multilineage repopulating activity. *J Exp Med*. 2011;208(12):2403-2416.
- Zhang Y, Stehling-sun S, Lezon-geyda K, et al. PR-domain – containing Mds1-Evi1 is critical for long-term hematopoietic stem cell function. *Blood*. 2011;118(14):3853-3861.
- Arber DA, Orazi A, Hasserjian R, et al. The 2016 revision to the World Health Organization classification of myeloid neoplasms and acute leukemia. *Blood*. 2016;127(20):2391-2405.
- Yamazaki H, Suzuki M, Otsuki A, et al. A remote GATA2 hematopoietic enhancer drives leukemogenesis in inv(3)(q21;q26) by activating EVI1 expression. *Cancer Cell*. 2014;25(4):415-427.
- Gröschel S, Sanders MA, Hoogenboezem R, et al. A single oncogenic enhancer rearrangement causes concomitant EVI1 and GATA2 deregulation in Leukemia. *Cell*. 2014;157(2):369-381.
- Smeenk L, Ottema S, Mulet-Lazaro R, et al. Selective requirement of MYB for oncogenic hyperactivation of a translocated enhancer in leukemia. *Cancer Discov*. 2021;11(11):2868-2883.
- Kiehmeier S, Rafiee MR, Bakr A, et al. Identification of therapeutic targets of the hijacked super-enhancer complex in EVI1-rearranged leukemia. *Leukemia*. 2021;35(11):3127-3138.
- Ottema S, Mulet-Lazaro R, Erpelinck-Verschueren C, et al. The leukemic oncogene EVI1 hijacks a MYC super-enhancer by CTCF-facilitated loops. *Nat Commun*. 2021;12(5679):1-13.
- Russell M, List A, Greenberg P, et al. Expression of EVI1 in myelodysplastic syndromes and other hematologic

- malignancies without 3q26 translocations. *Blood*. 1994;84(4):1243-1248.
15. Gröschel S, Schlenk RF, Engelmann J, et al. Deregulated expression of EVI1 defines a poor prognostic subset of MLL-rearranged acute myeloid leukemias: a study of the German-Austrian Acute Myeloid Leukemia Study Group and the Dutch-Belgian-Swiss HOVON/SAKK Cooperative Group. *J Clin Oncol*. 2013;31(1):95-103.
 16. Stavropoulou V, Kaspar S, Brault L, et al. MLL-AF9 expression in hematopoietic stem cells drives a highly invasive AML expressing EMT-related genes linked to poor outcome. *Cancer Cell*. 2016;30(1):43-58.
 17. Izutsu K, Kurokawa M, Imai Y, et al. The corepressor CtBP interacts with Evi-1 to repress transforming growth factor β signaling. *Blood*. 2001;97(9):2815-2822.
 18. Turner J, Crossley M. Cloning and characterization of mCtBP2, a co-repressor that associates with basic Kruppel-like factor and other mammalian transcriptional regulators. *EMBO J*. 1998;17(17):5129-5140.
 19. Ayoub E, Wilson MP, McGrath KE, et al. EVI1 overexpression reprograms hematopoiesis via upregulation of Spi1 transcription. *Nat Commun*. 2018;9(1):1-12.
 20. Wilson M, Tsakraklides V, Tran M, et al. EVI1 interferes with myeloid maturation via transcriptional repression of Cebpa, via binding to two far downstream regulatory elements. *J Biol Chem*. 2016;291(26):13591-13607.
 21. Cai SF, Chu SH, Goldberg AD, et al. Leukemia cell of origin influences apoptotic priming and sensitivity to LSD1 inhibition. *Cancer Discov*. 2020;10(10):1500-1513.
 22. Wang T, Birsoy K, Hughes NW, et al. Identification and characterization of essential genes in the human genome. *Science*. 2015;350(6264):1096-1101.
 23. Wang T, Yu H, Hughes NW, et al. Gene essentiality profiling reveals gene networks and synthetic lethal interactions with oncogenic Ras. *Cell*. 2017;168(5):1-14.
 24. Aguirre AJ, Meyers RM, Weir BA, et al. Genomic copy number dictates a gene-independent cell response to CRISPR-Cas9 targeting. *Cancer Discov*. 2016;6(8):914-929.
 25. Tzelepis K, Koike-Yusa H, De Braekeleer E, et al. A CRISPR dropout screen identifies genetic vulnerabilities and therapeutic targets in acute myeloid leukemia. *Cell Rep*. 2016;17(4):1193-1205.
 26. Meyers RM, Bryan JG, McFarland JM, et al. Computational correction of copy number effect improves specificity of CRISPR-Cas9 essentiality screens in cancer cells. *Nat Genet*. 2017;49(12):1779-1784.
 27. Morgens DW, Wainberg M, Boyle EA, et al. Genome-scale measurement of off-target activity using Cas9 toxicity in high-throughput screens. *Nat Commun*. 2017;8(1):15178.
 28. Behan FM, Iorio F, Picco G, et al. Prioritization of cancer therapeutic targets using CRISPR-Cas9 screens. *Nature*. 2019;568(7753):511-516.
 29. McFarland JM, Ho ZV, Kugener G, et al. Improved estimation of cancer dependencies from large-scale RNAi screens using model-based normalization and data integration. *Nat Commun*. 2018;9(1):1-13.
 30. Glass C, Wuertzer C, Cui X, et al. Global identification of EVI1 target genes in acute myeloid leukemia. *PLoS One*. 2013;8(6):e67134.
 31. Maicas M, Vázquez I, Vicente C, et al. Functional characterization of the promoter region of the human EVI1 gene in acute myeloid leukemia: RUNX1 and ELK1 directly regulate its transcription. *Oncogene*. 2013;32(16):2069-2078.
 32. Fenouille N, Bassil CF, Ben-Sahra I, et al. The creatine kinase pathway is a metabolic vulnerability in EVI1-positive acute myeloid leukemia. *Nat Med*. 2017;23(3):301-313.
 33. Hamaguchi H, Suzukawa K, Nagata K, et al. Establishment of a novel human myeloid leukaemia cell line (HNT-34) with t(3;3)(q21;q26), t(9;22)(q34;q11) and the expression of EVI1 gene, P210 and P190 BCR/ABL chimaeric transcripts from a patient with AML after MDS with 3q21q26 syndrome. *Br J Haematol*. 1997;98(2):399-407.
 34. de Almeida M, Hinterdorfer M, Brunner H, et al. AKIRIN2 controls the nuclear import of proteasomes in vertebrates. *Nature*. 2021;599(7885):491-496.
 35. Michlits G, Jude J, Hinterdorfer M, et al. Multilayered VBC score predicts sgRNAs that efficiently generate loss-of-function alleles. *Nat Methods*. 2020;17(7):708-716.
 36. Yokoyama A, Somerville TCP, Smith KS, et al. The menin tumor suppressor protein is an essential oncogenic cofactor for MLL-associated leukemogenesis. *Cell*. 2005;123(2):207-218.
 37. Lu B, Klingbeil O, Tarumoto Y, et al. A transcription factor addition in leukemia imposed by the MLL promoter sequence. *Cancer Cell*. 2018;34(6):970-981.e8.
 38. Tarumoto Y, Lu B, Somerville TDD, et al. LKB1, salt-inducible kinases, and MEF2C are linked dependencies in acute myeloid leukemia. *Mol Cell*. 2018;69(6):1017-1027.e6.
 39. Ohlsson E, Hasemann MS, Willer A, et al. Initiation of MLL-rearranged AML is dependent on C/EBP α . *J Exp Med*. 2014;211(1):5-13.
 40. Klaeger S, Heinzlmeier S, Wilhelm M, et al. The target landscape of clinical kinase drugs. *Science*. 2017;358(6367):eaan4368.
 41. Bard-Chapeau EA, Gunaratne J, Kumar P, et al. EVI1 oncoprotein interacts with a large and complex network of proteins and integrates signals through protein phosphorylation. *Proc Natl Acad Sci U S A*. 2013;110(31):E2885-E2894.
 42. Knudsen KJ, Rehn M, Hasemann MS, et al. ERG promotes the maintenance of hematopoietic stem cells by restricting their differentiation. *Genes Dev*. 2015;29(18):1915-1929.
 43. Unnikrishnan A, Guan YF, Huang Y, et al. A quantitative proteomics approach identifies ETV6 and IKZF1 as new regulators of an ERG-driven transcriptional network. *Nucleic Acids Res*. 2016;44(22):10644-10661.
 44. Cuenco GM, Nucifora G, Ren R. Human AML1/MDS1/EVI1 fusion protein induces an acute myelogenous leukemia (AML) in mice: a model for human AML. *Proc Natl Acad Sci U S A*. 2000;97(4):1760-1765.
 45. Nakamura Y, Ichikawa M, Oda H, et al. RUNX1-EVI1 induces dysplastic hematopoiesis and acute leukemia of the megakaryocytic lineage in mice. *Leuk Res*. 2018;74:14-20.
 46. Buonamici S, Li D, Chi Y, et al. EVI1 induces myelodysplastic syndrome in mice. *J Clin Invest*. 2004;114(5):713-719.
 47. Zuber J, Radtke I, Pardee TS, et al. Mouse models of human AML accurately predict chemotherapy response. *Genes Dev*. 2009;23(7):877-889.
 48. Schmoeller J, Barbosa IAM, Eder T, et al. CDK6 is an essential direct target of NUP98 fusion proteins in acute myeloid leukemia. *Blood*. 2020;136(4):387-400.
 49. Li Q, Haigis KM, McDaniel A, et al. Hematopoiesis and leukemogenesis in mice expressing oncogenic NrasG12D from the endogenous locus. *Blood*. 2011;117(6):2022-2032.
 50. Ottina E, Peperzak V, Schoeler K, et al. DNA-binding of the Tet-transactivator curtails antigen-induced lymphocyte activation in mice. *Nat Commun*. 2017;8(1):1028.
 51. Laurenti E, Frelin C, Xie S, et al. CDK6 levels regulate quiescence exit in human hematopoietic stem cells. *Cell Stem Cell*. 2015;16(3):302-313.
 52. Schleicher R, Hoelbl-Kovacic A, Bellutti F, et al. CDK6 as a key regulator of hematopoietic and leukemic stem cell activation. *Blood*. 2015;125(1):90-101.
 53. Klijn C, Durinck S, Stawiski EW, et al. A comprehensive transcriptional portrait of human cancer cell lines. *Nat Biotechnol*. 2015;33(3):306-312.
 54. Lavallée V-P, Gendron P, Lemieux SS, et al. EVI1-rearranged acute myeloid leukemias are characterized by distinct molecular alterations. *Blood*. 2015;125(1):140-143.
 55. Maiga A, Lemieux S, Pabst C, et al. Transcriptome analysis of G protein-coupled receptors in distinct genetic subgroups of acute myeloid leukemia: identification of potential disease-specific targets. *Blood Cancer J*. 2016;6(e431):1-9.
 56. Pabst C, Kros J, Fares I, et al. Identification of small molecules that support human leukemia stem cell activity ex vivo. *Nat Methods*. 2014;11(4):436-442.
 57. Celton M, Forest A, Gosse G, et al. Epigenetic regulation of GATA2 and its

- impact on normal karyotype acute myeloid leukemia. *Leukemia*. 2014;28(8):1617-1626.
58. Zuber J, Shi J, Wang E, et al. RNAi screen identifies Brd4 as a therapeutic target in acute myeloid leukaemia. *Nature*. 2011; 478(7370):524-528.
 59. Tzelepis K, De Braekeleer E, Aspris D, et al. SRPK1 maintains acute myeloid leukemia through effects on isoform usage of epigenetic regulators including BRD4. *Nat Commun*. 2018;9(5378):1-13.
 60. Tarumoto Y, Lin S, Wang J, et al. Salt-inducible kinase inhibition suppresses acute myeloid leukemia progression in vivo. *Blood*. 2020;135(1):56-70.
 61. Kucinski I, Wilson NK, Hannah R, et al. Interactions between lineage-associated transcription factors govern haematopoietic progenitor states. *EMBO J*. 2020;39(24):1-23.
 62. Roe JS, Mercan F, Rivera K, Pappin DJ, Vakoc CR. BET bromodomain inhibition suppresses the function of hematopoietic transcription factors in acute myeloid leukemia. *Mol Cell*. 2015;58(6):1028-1039.
 63. Kustikova OS, Schwarzer A, Stahlhut M, et al. Activation of Evi1 inhibits cell cycle progression and differentiation of hematopoietic progenitor cells. *Leukemia*. 2013;27(5):1127-1138.
 64. Thomas ME, Abdelhamed S, Hiltenbrand R, et al. Pediatric MDS and bone marrow failure-associated germline mutations in SAMD9 and SAMD9L impair multiple pathways in primary hematopoietic cells. *Leukemia*. 2021;35(11):3232-3244.
 65. Tesi B, Davidsson J, Voss M, et al. Gain-of-function SAMD9L mutations cause a syndrome of cytopenia, immunodeficiency, MDS, and neurological symptoms. *Blood*. 2017;129(16):1-4.
 66. Katayama S, Suzuki M, Yamaoka A, et al. GATA2 haploinsufficiency accelerates EVI1-driven leukemogenesis. *Blood*. 2017;130(7):908-919.
 67. Sankaran VG, Menne TF, Xu J, et al. Human fetal hemoglobin expression is regulated by the developmental stage-specific repressor BCL11A. *Science*. 2008;322(5909):1839-1842.
 68. Sunami Y, Yokoyama T, Yoshino S, et al. BCL11A promotes myeloid leukemogenesis by repressing PU.1 target genes. *Blood Adv*. 2022;6(6):1827-1843.
 69. Shields BJ, Jackson JT, Metcalf D, et al. Acute myeloid leukemia requires Hhex to enable PRC2-mediated epigenetic repression of Cdkn2a. *Genes Dev*. 2016; 30(1):78-91.
 70. Taoudi S, Bee T, Hilton A, et al. ERG dependence distinguishes developmental control of hematopoietic stem cell maintenance from hematopoietic specification. *Genes Dev*. 2011;25(3):251-262.
 71. Rockova V, Abbas S, Wouters BJ, et al. Risk stratification of intermediate-risk acute myeloid leukemia: integrative analysis of a multitude of gene mutation and gene expression markers. *Blood*. 2011;118(4):1069-1076.
 72. Zerkalenkova E, Panfyorova A, Kazakova A, et al. Molecular characteristic of acute leukemias with t(16;21)/FUS-ERG. *Ann Hematol*. 2018;97(6):977-988.
 73. Sotoca AM, Prange KHM, Reijnders B, et al. The oncofusion protein FUS-ERG targets key hematopoietic regulators and modulates the all-trans retinoic acid signaling pathway in t(16;21) acute myeloid leukemia. *Oncogene*. 2016;35(15):1965-1976.
 74. Weber S, Haferlach C, Jeromin S, et al. Gain of chromosome 21 or amplification of chromosome arm 21q is one mechanism for increased ERG expression in acute myeloid leukemia. *Genes Chromosomes Cancer*. 2016;55(2):148-157.
 75. Lee WY, Gutierrez-Lanz EA, Xiao H, et al. ERG amplification is a secondary recurrent driver event in myeloid malignancy with complex karyotype and TP53 mutations. *Genes Chromosomes Cancer*. 2022;61(7):399-411.
 76. Thoms JAI, Birger Y, Foster S, et al. ERG promotes T-acute lymphoblastic leukemia and is transcriptionally regulated in leukemic cells by a stem cell enhancer. *Blood*. 2011; 117(26):7079-7089.
 77. Masamoto Y, Chiba A, Mizuno H, et al. EVI1 exerts distinct roles in AML via ERG and cyclin D1 promoting a chemoresistance and immune-suppressive environment. *Blood Adv*. Published online 21 October 2022. <https://doi.org/10.1182/bloodadvances.2022.008018>
 78. Thirant C, Ignacimouttou C, Lopez CK, et al. ETO2-GLIS2 hijacks transcriptional complexes to drive cellular identity and self-renewal in pediatric acute megakaryoblastic leukemia. *Cancer Cell*. 2017;31(3):452-465.
 79. Tomlins SA, Rhodes DR, Perner S, et al. Recurrent fusion of *TMPRSS2* and *ETS* transcription factor genes in prostate cancer. *Science*. 2005;310(5748):644-648.
 80. Giovannini M, Biegel JA, Serra M, et al. EWS-erg and EWS-Fli1 fusion transcripts in Ewing's sarcoma and primitive neuroectodermal tumors with variant translocations. *J Clin Invest*. 1994;94(2):489-496.

© 2023 by The American Society of Hematology